Immunity, Volume *54*

Supplemental information

$CD8^+$ T cells specific for an immunodominant SARS-CoV-2 nucleocapsid epitope cross-react with selective seasonal coronaviruses

Katie E. Lineburg, Emma J. Grant, Srividhya Swaminathan, Demetra S.M. Chatzileontiadou, Christopher Szeto, Hannah Sloane, Archana Panikkar, Jyothy Raju, Pauline Crooks, Sweera Rehan, Andrea T. Nguyen, Lea Lekieffre, Michelle A. Neller, Zhen Wei Marcus Tong, Dhilshan Jayasinghe, Keng Yih Chew, Christian A. Lobos, Hanim Halim, Jacqueline M. Burrows, Alan Riboldi-Tunnicliffe, Weisan Chen, Lloyd D'Orsogna, Rajiv Khanna, Kirsty R. Short, Corey Smith, and Stephanie Gras

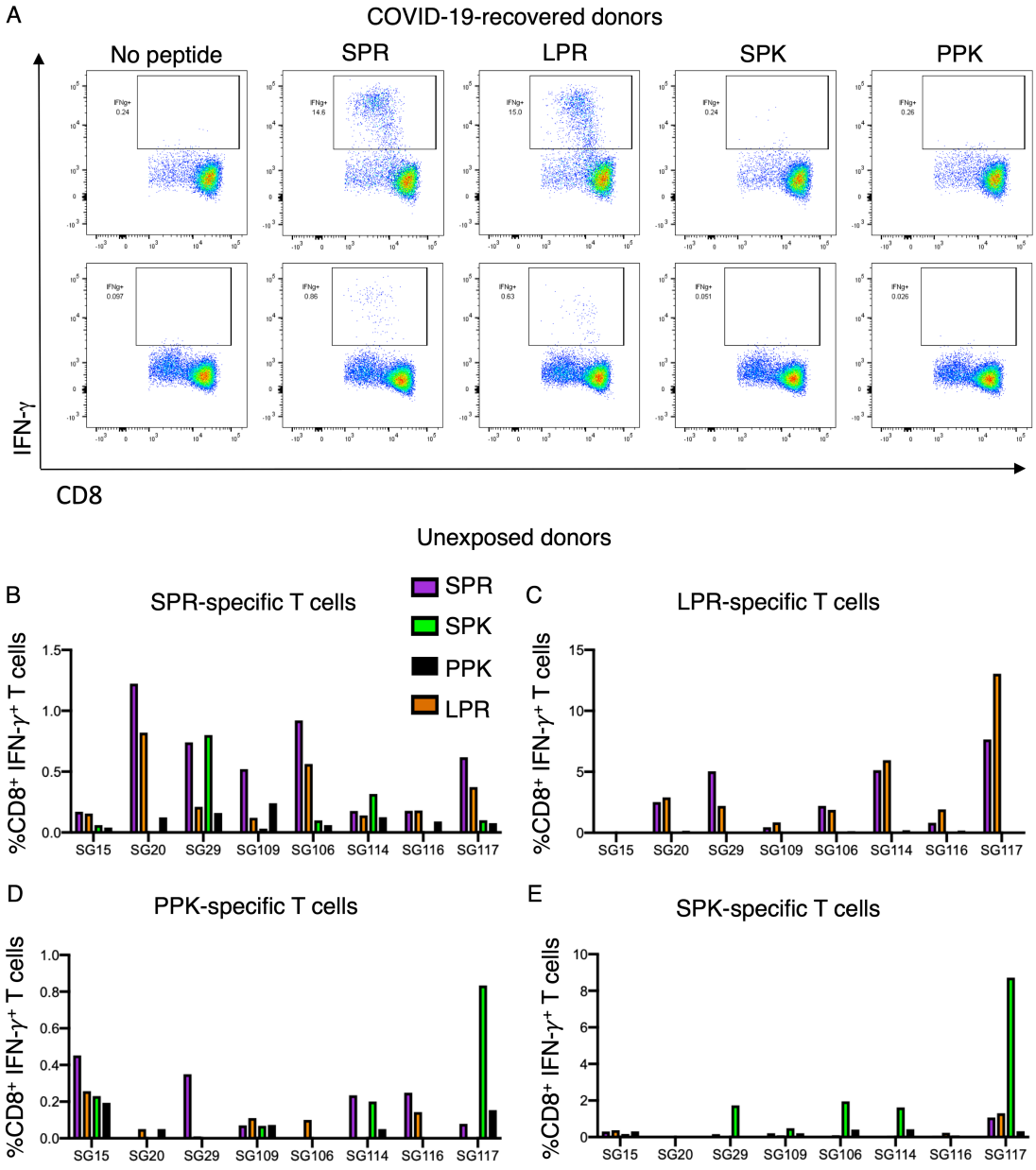

Figure S1. Cross-reactivity of SPR-specific CD8$^+$ T cells in COVID-19-recovered donors and from unexposed donors towards coronavirus peptides, Related to Figure 3.

(A) Following 14 days in culture, SPR-specific T cells were re-stimulated with five separate peptide conditions: no peptide control, cognate SPR, LPR, SPK or PPK and IFN-γ production was measured using an ICS assay. Representative flow cytometry displaying IFN-γ production in CD8$^+$ T cells generated from two separate COVID-19-recovered donors (top and bottom panels). (B-E) Peptide-specific CD8$^+$ T cells were expanded from unexposed donors (n=8) by stimulation with the (B) SPR, (C) LPR, (D) SPK or (E) PPK peptides and then re-stimulated separately with each peptide. The frequency of CD8$^+$ IFN-γ producing T cells was determined using an ICS assay. Summary of CD8$^+$ IFN-γ responses towards each of the variant peptides with the no peptide control subtracted.

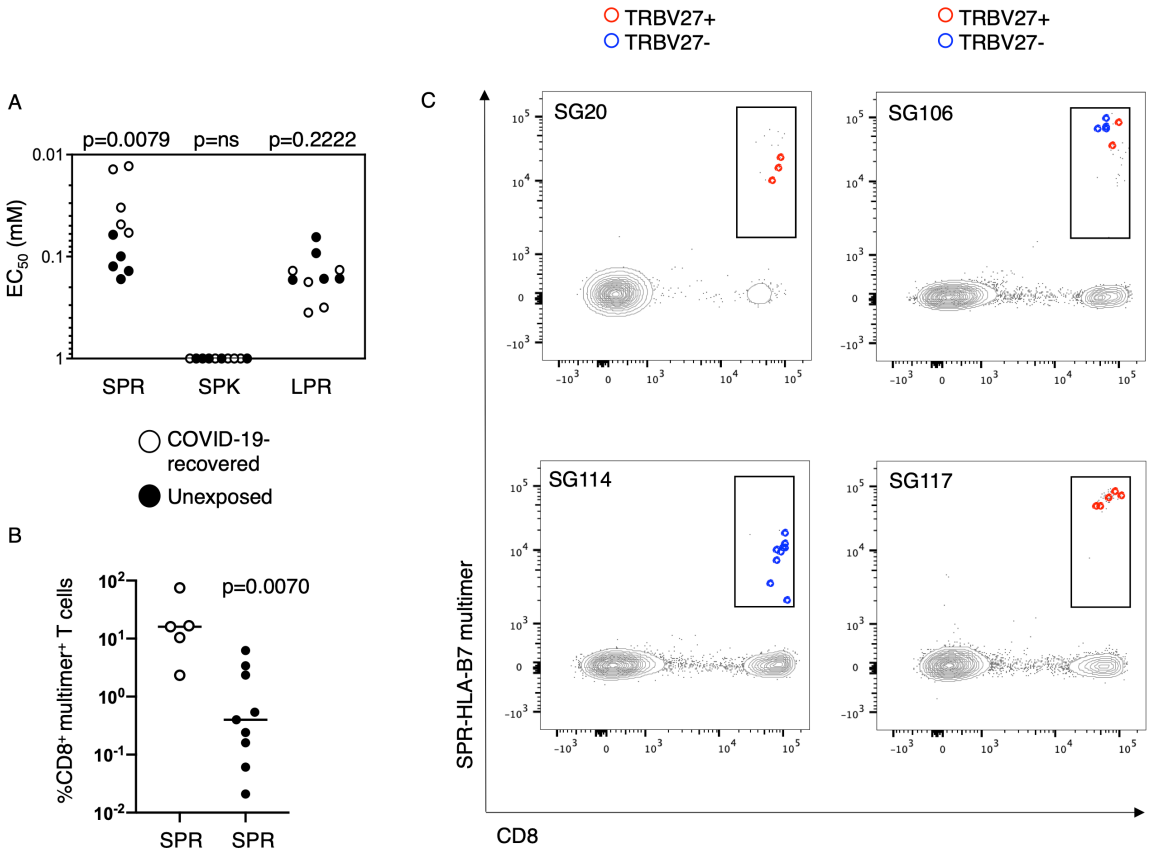

Figure S2. Functional avidity and magnitude of epitope-specific CD8$^+$ T cells from COVID-19-recovered and unexposed donors, and index sorting of SPR-specific T cells from unexposed donors, Related to Figure 3.

(A-B) Peptide-specific CD8$^+$ T cells were expanded from PBMCs derived from unexposed and COVID-19-recovered individuals. (A) Graph comparing the avidity (EC_{50}) of SPR-specific T cells derived from both COVID-19-recovered (white) and unexposed (black) individuals in response to cognate SPR peptide and homologous SPK and LPR peptides measured by IFN-γ production in an ICS assay. (B) Graph comparing the frequency of CD8$^+$ multimer$^+$ T cells between COVID-19 recovered (white) and unexposed (black) donors. The groups were compared using the Mann-Whitney test with $p < 0.05$ for significance, ns: non-significant. (C) SPR-specific CD8$^+$ T cells from unexposed donors were stained with SPR-HLA-B7 multimer and multimer$^+$CD8$^+$ cells were single-cell index sorted. A few clonotypes utilising TRBV27$^+$ (red) or TRBV27$^-$ (blue) overlaid on the total CD3$^+$/CD8$^+$ population are represented to show the wide range of functional avidities of the clones independently of the TRBV27 gene expression.

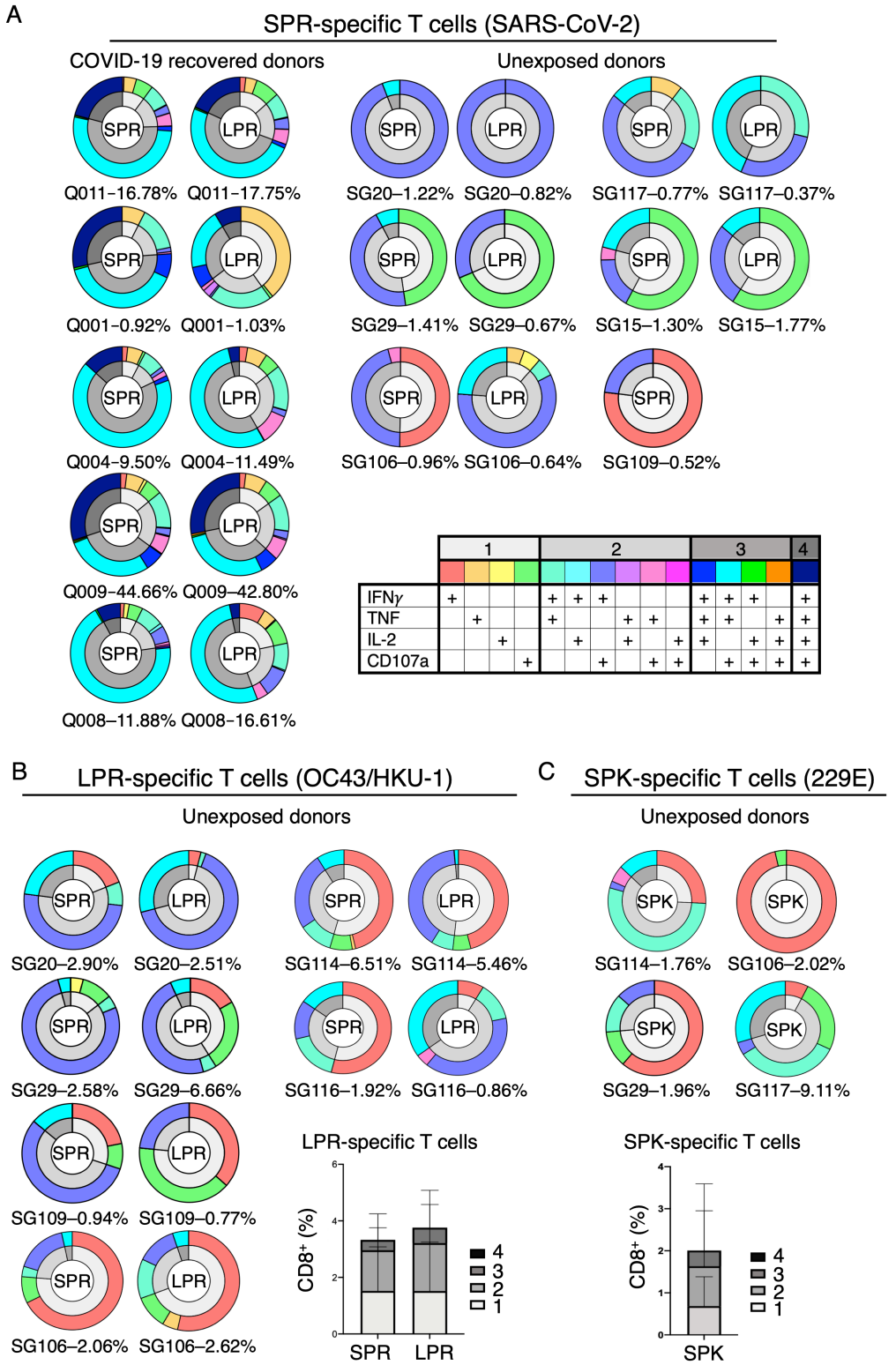

Figure S3. Polyfunctionality of SPR-specific CD8⁺ T cells from COVID-19-recovered and unexposed donors and LPR- and SPK-specific T cells from unexposed donors, Related to Figure 3.

(A) SPR-specific T cell lines were established from COVID-19-recovered (n=5) and unexposed donors (n=6), and re-stimulated individually with the SPR and LPR peptides in an ICS assay. (B) LPR- and (C) SPK-specific T cells were established and re-stimulated individually with the SPR, LPR, and SPK peptides in an ICS assay. The frequency of CD8⁺ T cells with different cytokine production profiles (IFN-γ, TNF,

IL-2 and CD107a) was determined, along with the number of different cytokines produced, minus the no peptide control. The outer ring of the double ring pie shows the cytokine profile in different colours, and the inner ring represents the number of cytokines produced with black for 4 and white for one.

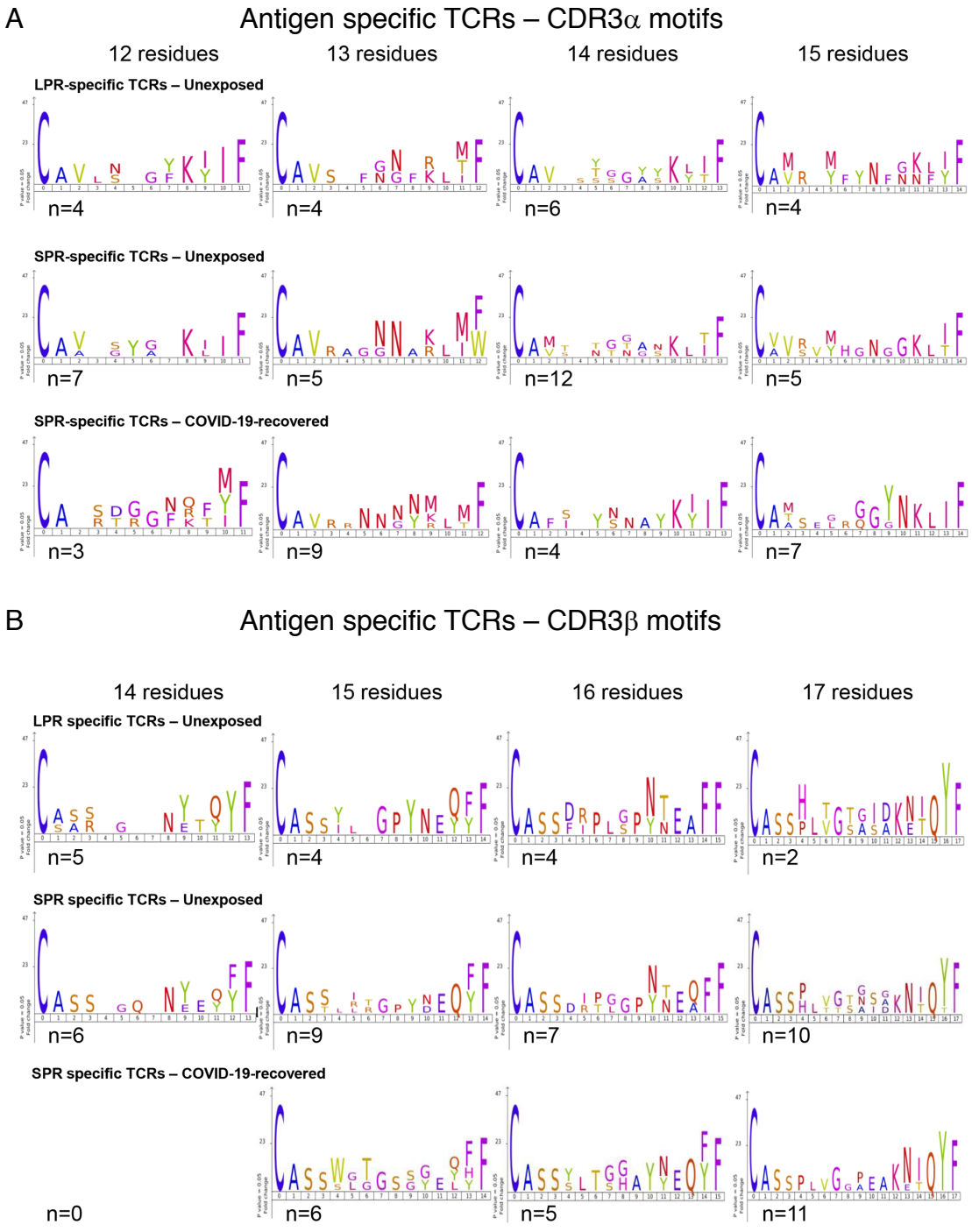

Figure S4. CDR3α and CDR3β analysis of the LPR- and SPR-specific CD8$^+$ T cells, Related to Figure 4.

PBMCs from COVID-19-recovered or unexposed individuals were stimulated with the SPK or LPR peptides and cultured for 10-14 days in the presence of IL2. CD8$^+$ T cell lines were stained with SPK or LPR multimer and multimer$^+$ cells were single-cell sorted and the TCR repertoire was determined by multiplex PCR. Analysis of the motifs of CDR3α and CDR3β sequences from distinct SPR and LPR-specific CD8$^+$ T cell clonotypes in unexposed and COVID-19-recovered individuals is shown.

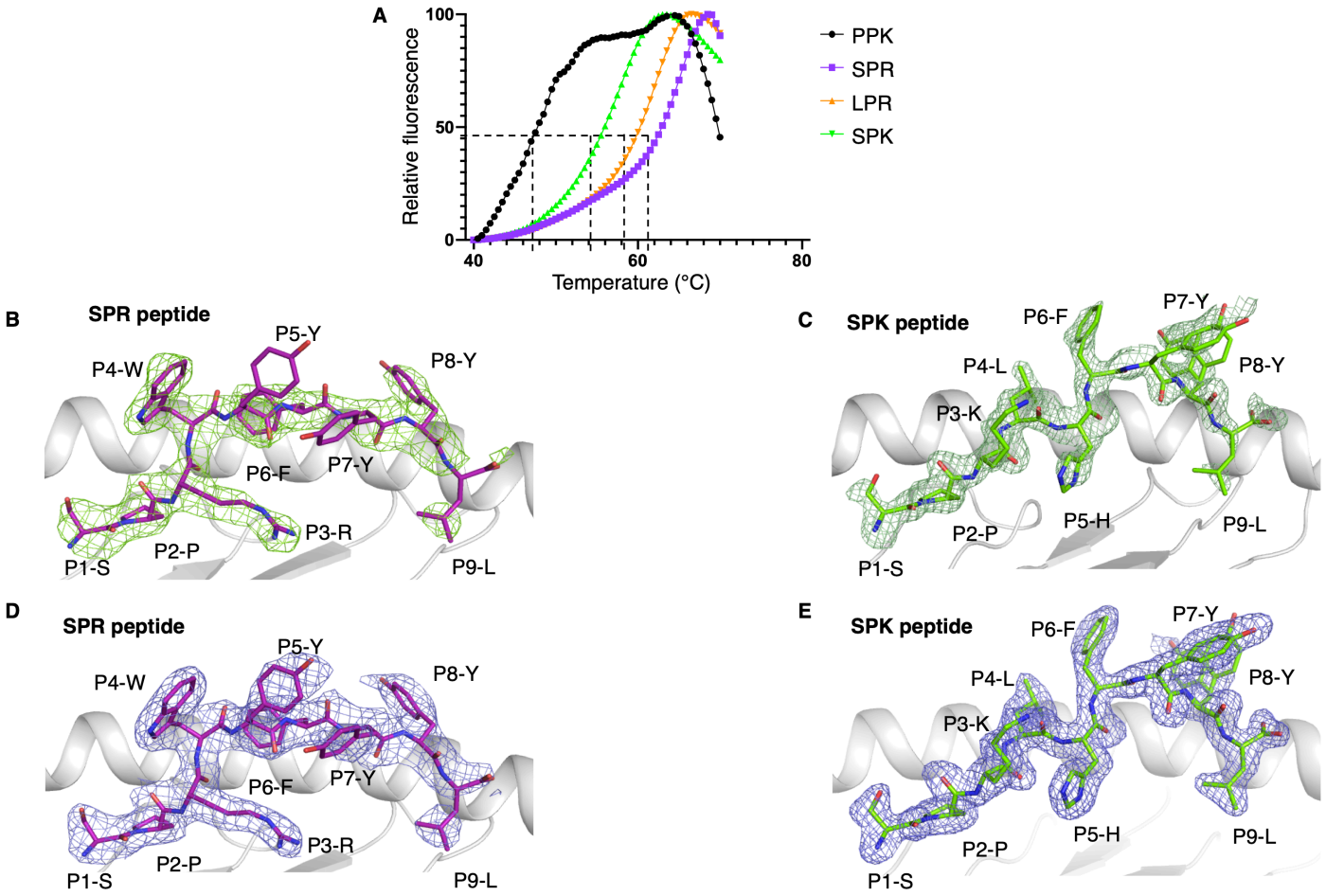

Figure S5. Thermal stability of HLA-B7 presenting coronaviruses peptides and electron density maps of the SPR and SPK peptides presented by HLA-B7, Related to Figure 5.

(**A**) Thermal stability profile of HLA-B7 in complex with coronavirus peptides derived from $N_{105\text{-}113}$ of viral strains SARS-CoV-2 (purple), or its homologous from NL63 (black), 229E (green) and OC43 (orange). Normalised fluorescence intensity follows a sigmoidal curve with an increase in temperature, as SYPRO Orange dye binds to exposed hydrophobic regions of pHLA-B7 during its thermal denaturation. The thermal midpoint temperature is determined at 50% of its normalised fluorescence intensity, allowing for the comparison of stability between pHLA-B7 complexes (summarised in **Table S4**). (**B-E**) HLA-B7 is represented as a white cartoon, the SPR peptide as purple sticks and the SPK peptide as green sticks. The **B** and **C** panels show the 2mFo-Fc electron density map, before building the peptide, contoured at 3σ and coloured in green, while the **D** and **E** panels show the Fo-Fc electron density maps, with the peptides build in and refinement cycles, contoured at 1σ and coloured in blue.

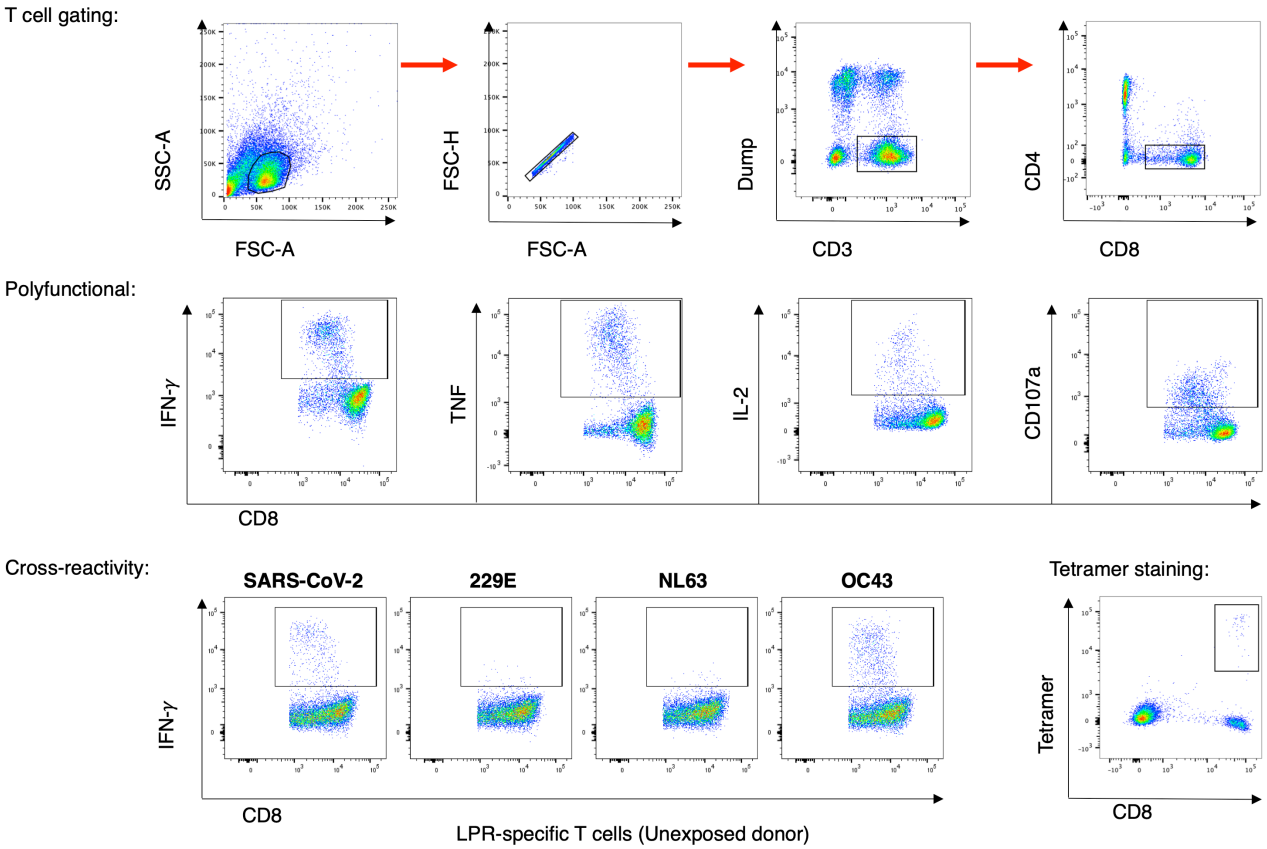

Figure S6. Gating strategy for our study, Related to Figures 1, 2, 3, and 4.
Peptide-specific $CD8^+$ T cells were derived by stimulating PBMCs from unexposed or COVID-19-recovered donors with various peptides as indicated throughout. $CD8^+$ T cell responses were subsequently assessed by either multimer staining or function in an ICS assay. Representative gating for the identification of $CD8^+$ T cells in all assays (top panel). Representative gating for the assessment of polyfunctionality (middle panel) or cross-reactivity (bottom panel, left) in an ICS assay. Representative flow cytometry plot of the identification of $multimer^+$ populations (bottom panel, right).

Table S1. HLA typing of COVID-19-recovered and unexposed donors, Related to Figures 1, 2, 3, and 4.

Donor ID	HLA-A	HLA-B	Age	Sex	Day post CoV PCR test
SG15	A*11:01, A*30:01	B*07:06, B*44:03	27	M	NA
SG20	A*32:01	B*07:02, B*44:02	32	F	NA
SG29	A*02:01, A*03:01	B*07:02, B*35:01	24	M	NA
SG105	A*02:01, A*29:02	B*07:02, B*44:03	N/A	N/A	NA
SG3	A*02:01, A*24:02	B*07:02, B*14:02	32	M	NA
SG34	A*02:01, A*24:02	B*07:02, B*08:01	24	F	NA
SG106	A*02:01, A*26:01	B*07:02, B*55:01	23	F	NA
SG109	A*02:01, A*26:01	B*07:02, B*44:02	19	F	NA
SG114	A*01:01, A*31:01	B*07:02, B*08:01	39	M	NA
SG116	A*03:01, A*29:02	B*07:02, B*44:03	32	F	NA
SG117	A*02:01, A*03:01	B*07:02, B*44:02	38	M	NA
GR001	A*01:01, A*03:01	B*07:02, B*08:01	42	M	NA
GR016	A*02:1	B*07:02	27	M	NA
GR036	A*02:01, A*03:01	B*07:02, B*44:02	40	F	NA
GR067	A*03:01	B*07:02	31	F	NA
GR082	A*01:01, A*02:01	B*07:02, B*44:02	56	M	NA
GR086	A*03:01	B*07:02	45	M	NA
Q001	A*03:01	B*07:02	20	M	58
Q002	A*02:01, A*32:01	B*15:01, B*44:02	53	F	49
Q003	A*01:01, A*25:01	B*08:01, B*35:01	52	M	53
Q004	A*02:01, A*03:01	B*07:02, B*44:02	30	F	51
Q005	A*02:01, A*11:01	B*15:01, B*35:01	33	M	58
Q006	A*02:01, A*24:02	B*07:02, B*18:01	48	M	48
Q007	A*02:01, A*31:01	B*07:02, B*40:01	20	F	53
Q008	A*02:01, A*03:01	B*07:02, B*44:02	48	F	58
Q009	A*03:01, A*26:01	B*07:02, B*27:05	63	F	62
Q010	A*02:01	B*15:01, B*44:03	63	M	49

Q011	A*02:01	B*07:02, B*44:02	59	F	67
Q012	A*02:01, A*03:01	B*44:02, B*51:01	71	F	53
Q013	A*24:02, A*25:01	B*08:01	51	F	54
Q014	A*03:01, A*29:02	B*07:02, B*44:03	61	F	54
Q015	A*02:01	B*35:03	30	F	46
Q016	A*03:03, A*24:03	B*35:01, B*38:01	25	F	71
Q017	A*03:01, A*26:01	B*07:02	58	F	102
Q018	A*02:05, A*30:01	B*13:02, B*49:01	63	M	102
Q019	A*01:01, A*24:02	B*08:01, B*27:05	60	F	59
Q020	A*24:02, A*31:01	B*07:02, B*35:02	58	M	58
Q021	A*01:01, A*24:02	B*08:01, B*35:02	26	F	56
Q022	A*01:01, A*31:01	B*07:02, B*08:01	21	F	57
Q024	A*01:01, A*03:01	B*07:02, B*08:01	56	F	83
Q025	A*01:01, A*02:01	B*08:01, B*40:01	67	F	67
Q026	A*01:01, A*30:02	B*40:01, B*49:01	39	F	61
Q029	A*02:01, A*31:02	B*07:02, B*40:01	31	F	69
Q031	A*02:01, A*29:02	B*15:01, B*44:03	61	M	85
Q032	A*02:01	B*27:05, B*44:02	25	F	70
Q033	A*02:01, A*24:02	B*15:01, B*18:04	25	M	76
Q035	A*02:01, A*03:01	B*07:02, B*08:01	62	F	76
Q038	A*01:01, A*02:01	B*08:01, B*44:02	41	F	88
Q040	A*02:01, A*32:01	B*44:02, B*44:03	74	F	82
Q045	A*01:01, A*03:01	B*07:02, B*14:02	21	F	67
Q046	A*02:01, A*24:02	B*15:01, B*40:01	44	M	80
Q049	A*01:01, A*03:01	B*07:02, B*56:01	51	M	116
Q052	A*01:01, A*24:02	B*07:02, B*44:03	67	M	75
Q062	A*02:01	B*08:01, B*18:01	22	F	124

All donors with ID SG or GR are unexposed donors, all donors with ID Q0 are COVID-19-recovered donors, M: male, F: female.

Table S2. COVID-19 symptoms and classification, Related to Figures 1, 2, 3, and 4.

HLA-B7^{+} donor ID	**Symptom classification**	**Symptoms included**
Q001	Other	FE|CO|SO|HE|LO|SK|GA
Q004	Mild	HE|LO|OT
Q006	Severe	CO|SH|SO|HE|LO|JO|GA
Q007	NA	NA
Q008	Moderate	CO|SH|SO|HE|SK|GA
Q009	Mild	CO
Q011	Severe	SO|HE|LO|OT
Q014	Mild	FE|CO|HE|LO|GA
Q017	Mild	SO|HE|OT
Q020	Moderate	FE|CO|SH|HE|LO|JO|OT
Q022	Mild	CO|SO|LO|JO|OT
Q029	NA	NA
Q035	Moderate	FE|CO|SH|SO|OT
Q045	NA	NA
Q049	Mild	SO|HE
Q052	Mild	OT
HLA-B7^{-} donor ID	**Symptom classification**	**Symptoms included**
Q002	Mild	CO|LO|OT
Q003	Mild	CO|HE|JO
Q005	Severe	CO|SH|SO|HE|JO|OT
Q010	Mild	FE|CO|LO|GA
Q012	NA	NA
Q013	Mild	LO|OT
Q015	NA	NA
Q016	Mild	HE|OT
Q018	Mild	CO|SO|OT
Q019	Mild	SO|HE|LO|JO|OT
Q021	NA	NA
Q025	NA	NA

Q026	Mild	FE|CO|HE|LO|GA|OT
Q031	Mild	FE|CO
Q032	Moderate	FE|CO|SH|HE|LO|GA|OT
Q033	NA	NA
Q038	Moderate	FE|SH|HE|LO|GA
Q040	Severe	FE|HE|LO|JO|GA
Q046	NA	NA
Q062	Mild	LO|OT

FE: fever; CO: cough; SO: Sore throat; SH: Short of breath; HE: headache; LO: Loss of taste or smell; JO: Joint pain; GA: Gastrointestinal symptoms; OT: other; SK: Skin rash.

Table S3. HLA-B7-resticted epitopes defined in SARS-CoV-2 nucleocapsid, Related to Figures 1 and 2.

Peptide origin	Peptide name	Peptide sequence	Number of Responders*
N_{66-74}	FPR	FPRGQGVPI	1 / 17
N_{93-101}	RIR	RIRGGDGKM	4 / 17
$N_{105-113}$	SPR	SPRWYFYYL	14 / 17
$N_{257-265}$	KPR	KPRQKRTAT	1 / 17

*Responders are COVID-19-recovered HLA-B7^{+} individuals.

Table S4. Sequence variation in coronaviruses isolates of the SPR peptide and homologues, Related to Figure 3.

Virus	Sequence	Oceania	Asia	Europe	Africa	North America	South America	Total number of sequences
SARS-CoV-2	SPRWYFYYL	100% (8,693)	100% (1,330)	100% (438)	100% (281)	100% (15,273)	100% (143)	26,158
SARS-CoV-1	SPRWYFYYL	NA	100% (2)	NA	NA	100% (11)	NA	13
OC43	LPRWYFYYL	NA	100% (61)	100% (3)	100% (3)	100% (69)	NA	136
HKU-1	LPRWYFYYL	NA	100% (3)	100% (1)	NA	100% (12)	NA	16
229E	SPKLHFYYL	NA	NA	100% (3)	NA	100% (23)	NA	26
NL63	PPKVHFYYL	NA	100% (8)	NA	100% (7)	100% (43)	NA	58

Complete full length sequences were obtained from the NCBI virus database http://www.ncbi.nlm.nih,gov/labs/virus and were aligned using https://www.fludb.org/brc/home.spg?decorator=influenza. The frequency of peptide conservation is shown in green, with the number of sequences aligned from each geographic region shown in parenthesis. Mutations from the SARS-CoV-2 peptide are denoted in blue, and anchor residues are underlined. NA refers to no sequences being available for that geographic region.

Table S6. Data collection and refinement statistics, Related to Figure 5.

Data Collection Statistics	**HLA-B7-SPR**	**HLA-B7-SPK**
Space group	**$P2_12_12_1$**	**P1**
Cell Dimensions (a,b,c) (Å)	64.45, 107.18, 174.19	57.14, 62.85, 63.01 α=77.15°, β=77.00°, γ=77.86°
Resolution (Å)	46.65 – 2.88 (3.04 – 2.88)	44.53 – 1.97 (2.02 – 1.97)
Total number of observations	191654 (26453)	204851 (14311)
Nb of unique observation	28141 (4027)	56880 (3904)
Multiplicity	6.8 (6.6)	3.6 (3.7)
Data completeness (%)	100 (100)	98.1 (96.8)
I/σ_I	8.0 (1.6)	5.5 (1.7)
R_{pim}[a] (%)	8.0 (52.9)	7.4 (43.8)
$CC_{1/2}$ (%)	89.8 (57.8)	99.0 (55.2)
Refinement Statistics		
R_{factor}[b] (%)	20.6	18.6
R_{free}[b] (%)	26.9	23.0
rmsd from ideality		
Bond lengths (Å)	0.009	0.008
Bond angles (°)	1.038	0.955
Ramachandran plot (%)		
Favoured	96.3	97.9
Allowed	3.6	1.7
Disallowed	0.1	0.4
PBD code	**7LGD**	**7LGT**

[a]$R_{p.i.m} = \Sigma_{hkl} [1/(N-1)]^{1/2} \Sigma_i | I_{hkl,\,i} - \langle I_{hkl} \rangle | / \Sigma_{hkl} \langle I_{hkl} \rangle$. [b]$R_{factor} = \Sigma_{hkl} \; | \, | F_o | - | F_c | \, | / \Sigma_{hkl} | F_o |$ for all data except ≈ 5% which were used for R_{free} calculation. Values in parentheses are for the highest resolution-shell.